

Study of the critical point in lattice QCD at high temperature and density

Shinji Ejiri^{*†}

Physics Department, Brookhaven National Laboratory, Upton, New York 11973, USA

E-mail: ejiri@quark.phy.bnl.gov

We propose a method to probe the nature of phase transitions in lattice QCD at finite temperature and density, which is based on the investigation of an effective potential as a function of the average plaquette. We analyze data obtained in a simulation of two-flavor QCD using p4-improved staggered quarks with bare quark mass $m/T = 0.4$, and find that a first order phase transition line appears in the high density regime for $\mu_q/T \gtrsim 2.5$. The effective potential as a function of the quark number density is also studied. We calculate the chemical potential as a function of the density from the canonical partition function and discuss the existence of the first order phase transition line.

The XXV International Symposium on Lattice Field Theory

July 30 - August 4 2007

Regensburg, Germany

^{*}Speaker.

[†]This work has been authored under contract DE-AC02-98CH1-886 with the U.S. Department of Energy.

1. Effective potential as a function of the average plaquette

The study of the QCD phase diagram at non-zero temperature (T) and chemical potential (μ_q) is one of the most important topics among studies of lattice QCD. In particular, the study of the endpoint of the first order phase transition line in the (T, μ_q) plane is particularly interesting both from the experimental and theoretical point of view. The existence of such a critical point is suggested by phenomenological studies. The appearance of the critical endpoint in the (T, μ_q) plane is closely related to hadronic fluctuations in heavy ion collisions and may be experimentally examined by an event-by-event analysis of heavy ion collisions. Many trials have been made to prove the existence of the critical endpoint by first principle calculation in lattice QCD, however no definite conclusion on this issue is obtained so far. The purpose of this study is to clarify the existence of the endpoint of the first order phase transition line in the (T, μ_q) plane. We propose a new method to investigate the nature of transition.

We evaluate an effective potential as a function of the average plaquette (P)¹, and identify the type of transition from the shape of the potential. The partition function can be written as²

$$\mathcal{Z}_{\text{GC}}(\beta, \mu_q) = \int \mathcal{D}U (\det M(\mu_q))^{N_f} e^{-S_g(P, \beta)} = \int R(P, \mu_q) w(P) e^{-S_g(P, \beta)} dP, \quad (1.1)$$

where $S_g(P, \beta)$ is the gauge action, $w(P)$ is the state density at $\mu_q = 0$ for each P ,

$$w(P') e^{-S_g(P', \beta)} \equiv w(P', \beta) \equiv \int \mathcal{D}U \delta(P' - P) (\det M)^{N_f} e^{6\beta N_{\text{site}} P}, \quad (1.2)$$

and $R(P, \mu_q)$ is the modification (reweighting) factor for finite μ_q , which is defined by

$$R(P', \mu_q) \equiv \frac{\int \mathcal{D}U \delta(P' - P) (\det M(\mu_q))^{N_f}}{\int \mathcal{D}U \delta(P' - P) (\det M(0))^{N_f}} = \frac{\langle \delta(P' - P) (\det M(\mu_q) / \det M(0))^{N_f} \rangle_{(\beta, \mu_q=0)}}{\langle \delta(P' - P) \rangle_{(\beta, \mu_q=0)}} \quad (1.3)$$

where $\langle \cdots \rangle_{(\beta, \mu_q=0)}$ means the expectation value at $\mu_q = 0$, $\det M$ is the quark determinant, N_f is the number of flavors³, and $N_{\text{site}} = N_s^3 \times N_f$ is the number of sites. We then define the effective potential as $V(P, \beta, \mu_q) = -\ln(Rw e^{-S_g})$. If there is a first order phase transition point, where two different states coexist, the potential must have two minima at two different values of P . In this paper, we discuss whether the potential at $\mu_q = 0$, i.e. $\ln(w e^{-S_g})$, which is quadratic function when the transition is a crossover, can change to a double-well potential by the reweighting factor for finite μ_q , as illustrated in Fig. 1 (left).

2. Taylor expansion in terms of μ_q/T and Gaussian distribution

However, the calculation of the quark determinant is quite expensive and is actually difficult except on small lattices. Moreover, the calculation of $R(P, \mu_q)$ becomes increasingly more difficult

¹For later discussions, we define the average plaquette P as $P \equiv -S_g / (6\beta N_{\text{site}})$. This is the average of the plaquette over all elementary squares for the standard gauge action.

²We restrict ourselves to discuss only the case when the quark matrix does not depend on β explicitly, e.g. the standard Wilson and staggered quark actions, the p4-improved staggered quark action etc., for simplicity.

³ N_f must be replaced in these equations to $N_f/4$ when we use a staggered type quark action.

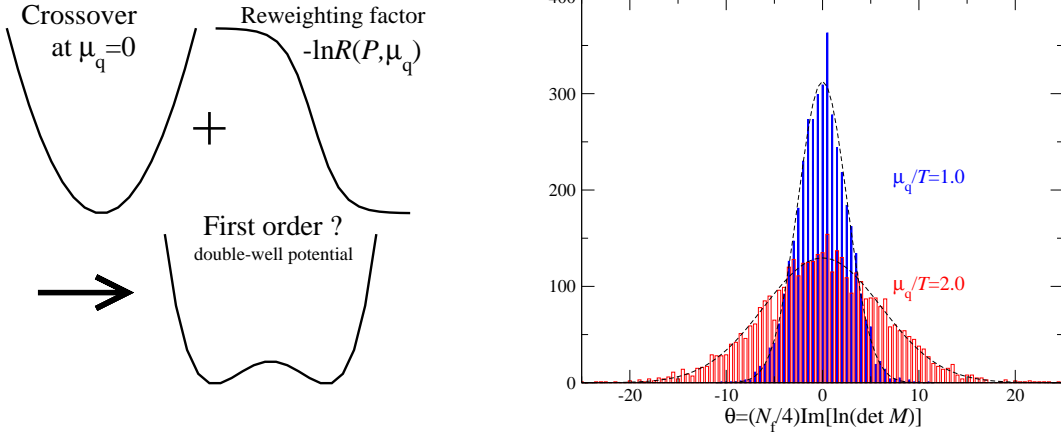


Figure 1: (left) Schematic figures of the effective potential and the reweighting factor. (right) The histogram of the complex phase for $\mu_q/T = 1.0$ and 2.0 at $\beta = 3.65$.

for large μ_q due to the sign problem, i.e. the statistical error becomes exponentially larger as μ_q increases. We avoid these problems by the following two ideas. One is that we perform a Taylor expansion of $\ln \det M(\mu_q)$ in terms of μ_q at $\mu_q = 0$ and calculate the expansion coefficients [1],

$$\ln \left[\frac{\det M(\mu_q)}{\det M(0)} \right] = \sum_{n=1}^{\infty} \frac{1}{n!} \left[\frac{\partial^n (\ln \det M)}{\partial (\mu_q/T)^n} \right] \left(\frac{\mu_q}{T} \right)^n \equiv N_s^3 N_t \sum_{n=1}^{\infty} D_n \left(\frac{\mu_q}{T} \right)^n. \quad (2.1)$$

The Taylor expansion coefficients are rather easy to calculate by using the stochastic noise method. Although we must cut off this expansion at an appropriate order in μ_q , we can estimate the application range where the approximation is valid for each analysis [2, 3]. While the application range of the Taylor expansion of $\ln \mathcal{L}_{GC}$ should be limited by the critical point because $\ln \mathcal{L}_{GC}$ is singular at the critical point, there is no such limit for the application range in the expansion of $\ln R(P, \mu_q)$ because the weight factor should always be well-defined.

The sign problem is avoided by the following idea. We consider a probability distribution function as a function of the complex phase of the quark determinant θ , $|F| \equiv |\det M(\mu_q) / \det M(0)|^{N_f}$ and P , i.e. $\bar{w}(P, |F|, \theta)$. If we assume the distribution function in θ is well-approximated by a Gaussian function, the sign problem in the calculation of $\ln R(P, \mu_q)$ is completely solved [4].

We define the complex phase by a Taylor expansion, $\theta = N_f N_s^3 N_t \sum_{n=0}^{\infty} \text{Im} D_{2n+1} (\mu_q/T)^{2n+1}$. Since the partition function is real even at non-zero density, the distribution function has the symmetry under the change from θ to $-\theta$. Therefore, the distribution function is written by $\bar{w}(\theta) \sim \exp[-(a_2 \theta^2 + a_4 \theta^4 + a_6 \theta^6 + \dots)]$. Moreover, because D_n is a trace of a matrix which has space index [3], e.g. $D_1 \propto \text{tr}[M^{-1} dM/d(\mu_q/T)]$, the central limit theorem suggests that the distribution function is well-approximated by a Gaussian function, when the system size is sufficiently large in comparison to the correlation length between diagonal elements of the matrix. We plotted the distribution of the complex phase in Fig. 1 (right) and fitted by a Gaussian function (dashed line). It is found that this approximation is quite well, hence we consider the leading term of the expansion only, $\bar{w}(P, |F|, \theta) \propto \sqrt{a_2(P, |F|)/\pi} \exp[-a_2(P, |F|)\theta^2]$. The coefficient $a_2(P, |F|)$

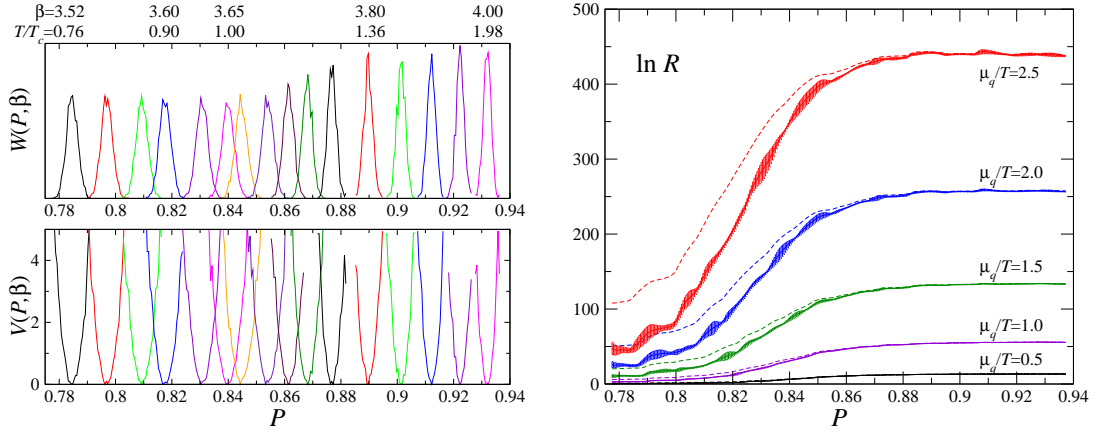


Figure 2: (left) The plaquette histogram and the effective potential at $\mu_q = 0$. (right) The reweighting factor $\ln R(P, \mu_q)$ for $\mu_q/T = 0.5 - 2.5$.

is given by $1/(2a_2) = \langle \theta^2 \rangle$ for each P and $|F|$. The numerator of Eq. (1.3) is then evaluated by

$$\langle F(\mu_q) \delta(P' - P) \rangle_{(\beta, \mu_q=0)} \approx \left\langle e^{-1/(4a_2(P, |F|))} |F(\mu_q)| \delta(P' - P) \right\rangle_{(\beta, \mu_q=0)}. \quad (2.2)$$

Because $1/a_2 \sim O(N_{\text{site}})$, the phase factor in $R(P, \mu_q)$ decreases exponentially as a function of the volume. However, the operator in Eq. (2.2) is always real and positive for each configuration in this framework, hence the expectation value of $R(P, \mu_q)$ is always larger than its statistical error, namely the contribution $\ln R(P, \mu_q)$ to the effective potential $V(P, \beta, \mu_q)$ is always well-defined. Therefore, the sign problem is completely avoided if we can assume the Gaussian distribution of θ .

3. Numerical results of the effective potential

We calculate $w(P, \beta)$ and $R(P, \mu_q)$ using data obtained by simulations in [3]. The Taylor expansion coefficients are computed up to $O(\mu_q^6)$. These are measured at sixteen simulation points from $\beta = 3.52$ to 4.00 for the bare quark mass $ma = 0.1$. The corresponding temperature normalized by the pseudo-critical temperature is in the range of $T/T_c = 0.76$ to 1.98 . The ratio of pseudo-scalar and vector meson masses is $m_{\text{PS}}/m_{\text{V}} \approx 0.7$ at $\beta = 3.65$. The lattice size N_{site} is $16^3 \times 4$. The number of configurations is 1000 – 4000 for each β .

The probability distribution function $w(P, \beta)$, i.e. the histogram of P for each β , and the effective potential $V(P, \beta)$ at $\mu_q = 0$ are given in Fig. 2(left). To obtain $w(P, \beta)$, we grouped the configurations by the value of P into blocks and counted the number of configurations in these blocks, and the potential $V(P, \beta)$ is normalized by the minimum value for each temperature.

The results for $\ln R(P, \mu_q)$ are shown by solid lines in Fig. 2 (right) for $\mu_q/T = 0.5, 1.0, 1.5, 2.0$ and 2.5 . We find a rapid change in $\ln R$ around $P \sim 0.83$, and the variation becomes larger as μ_q/T increases. The dashed lines in Fig. 2 (right) are the results that we obtained when the effect of the complex phase, i.e. $\exp[-1/(4a_2)]$, is omitted. These dashed lines correspond to the reweighting factor with non-zero isospin chemical potential μ_I and zero quark chemical potential μ_q [5]. The variation of $\ln R$ in terms of P becomes milder when the effect of the complex phase is omitted.

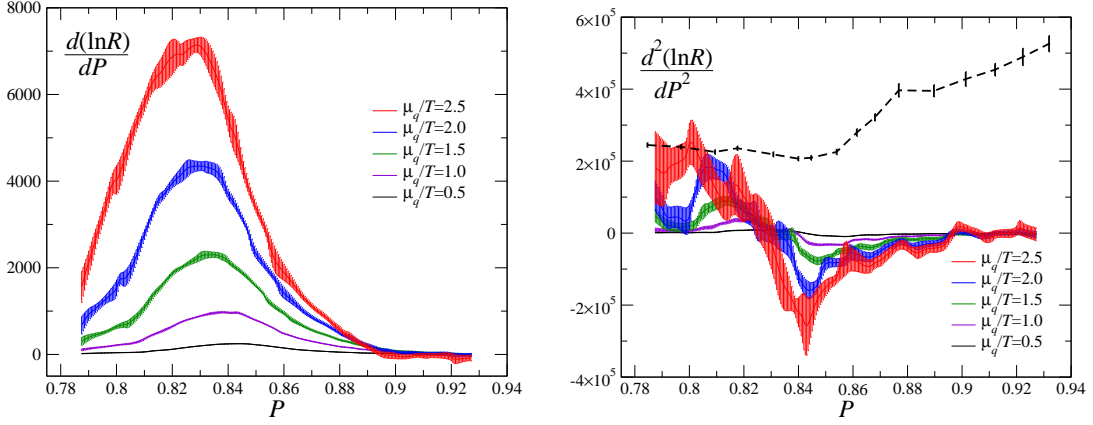


Figure 3: The slope (left) and curvature (right) of $\ln R(P, \mu_q)$. The dashed line is the curvature of $-\ln w$.

This explains the difference between the phase diagrams of QCD with non-zero quark chemical potential and non-zero isospin chemical potential [4].

We discuss the shape of the effective potential at non-zero μ_q . The effective potential is obtained from $V(P, \beta, \mu_q) = -\ln w(P, \beta) - \ln R(P, \mu_q)$ substituting the data in Fig. 2. From Eq. (1.2), the slope of $V(P, \beta, \mu_q)$ can be controlled by β ,

$$V(P, \beta, \mu_q) = V(P, \beta_0, \mu_q) - 6(\beta - \beta_0)N_{\text{site}}P. \quad (3.1)$$

under a change of $\beta_0 \rightarrow \beta$, however the curvature of the potential does not change by β . We expect that the curvature vanishes at the endpoint of the first order phase transition line by canceling $d^2(\ln w)/dP^2$ and $d^2(\ln R)/dP^2$. In order to analyze the sign of $d^2V/dP^2(P, \mu_q)$, we fitted the data of $\ln R$ by a quadratic function of P and calculate the first and second derivatives of $\ln R(P, \mu_q)$ at each P . The results of the slope and curvature are shown in Fig. 3 for each μ_q/T . In the region around $P \sim 0.83$, $d(\ln R)/dP$ becomes larger as μ_q/T increases and $\ln R(P, \mu_q)$ changes sharply in this region. The magnitude of the curvature of $\ln R$ also becomes larger as μ_q/T increases.

To evaluate $d^2(\ln w)/dP^2(P)$, we assume $w(P, \beta)$ in Fig. 2 (left) is a Gaussian function. In this case, the curvature at $\langle P \rangle$ is given by $-d^2(\ln w)/dP^2 = 6N_{\text{site}}/\chi_P$, where $\chi_P \equiv 6N_{\text{site}}\langle(P - \langle P \rangle)^2\rangle$ is the plaquette susceptibility. The dashed line in Fig. 3 (right) is the result of $-d^2(\ln w)/dP^2(P)$.

It is found from Fig. 3 (right) that the maximum value of $d^2(\ln R)/dP^2(P, \mu_q)$ at $P = 0.80$ becomes larger than $-d^2(\ln w)/dP^2$ for $\mu_q/T \gtrsim 2.5$. This means that the curvature of the effective potential vanishes at $\mu_q/T \sim 2.5$ and becomes negative for large μ_q/T , namely the shape of the effective potential which is of quadratic type at $\mu_q = 0$ changes to a double-well type at large μ_q/T . For the quantitative estimation of the endpoint of the first order phase transition, further investigation must be needed. However, this argument strongly suggests the existence of the first order phase transition line in the (T, μ_q) plane. Further details of this analysis are given in [4].

4. Canonical partition function

Next, we want to apply the effective potential argument to the weight factor as a function of the quark number density ρ . The physical meaning of this potential is clearer than that of P because

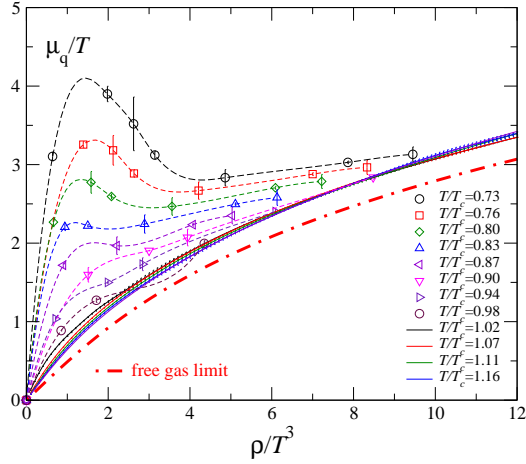


Figure 4: The chemical potential as a function of the quark number density.

the weight factor for each quark number N corresponds to the canonical partition function \mathcal{Z}_C ,

$$\mathcal{Z}_{GC}(T, \mu_q) = \sum_N e^{N\mu_q/T} \mathcal{Z}_C(T, N), \quad N = \bar{\rho} N_s^3, \quad \rho/T^3 = \bar{\rho} N_t^3. \quad (4.1)$$

The canonical partition function can be given by an inverse Laplace transformation [6, 7, 8],

$$\mathcal{Z}_C(T, N) = \frac{3}{2\pi} \int_{-\pi/3}^{\pi/3} d(\mu_I/T) e^{-N(\mu_0/T + i\mu_I/T)} \mathcal{Z}_{GC}(T, \mu_0 + i\mu_I), \quad (4.2)$$

where μ_0 is an appropriate real constant. Note that $\mathcal{Z}_{GC}(T, \mu_q + 2\pi i T/3) = \mathcal{Z}_{GC}(T, \mu_q)$. Recently, this canonical partition function is calculated for $N_f = 4$ using the Glasgow method [9]. However, with present day computer resources, the calculation by the Glasgow method is difficult except on small lattices. We consider approximations which is valid for large volume and low density in this approach, as discussed in the first part of this paper.

We calculate the grand partition function by the Taylor expansion, Eq. (2.1),

$$\frac{\mathcal{Z}_{GC}(T, \mu_q)}{\mathcal{Z}_{GC}(T, 0)} = \frac{1}{\mathcal{Z}_{GC}} \int \mathcal{D}U \left(\frac{\det M(\mu_q)}{\det M(0)} \right)^{N_f} (\det M(0))^{N_f} e^{-S_g} \equiv \left\langle e^{[N_f N_t V \sum_{n=1}^{\infty} D_n (\frac{\mu_q}{T})^n]} \right\rangle_{(T, \mu_q=0)}, \quad (4.3)$$

where $V \equiv N_s^3$. We moreover use a saddle point approximation, which is valid for a large system. We find a saddle point z_0 in the complex μ_q/T plane for each configuration, which satisfies $[N_f N_t \sum_{n=1}^{\infty} n D_n z_0^{n-1} - \bar{\rho}]_{z=z_0} = 0$. The canonical partition function is given by

$$\mathcal{Z}_C(T, \bar{\rho}V) \approx \frac{3}{\sqrt{2\pi}} \mathcal{Z}_{GC}(T, 0) \left\langle \exp \left[V \left(N_f N_t \sum_{n=1}^{\infty} D_n z_0^n - \bar{\rho} z_0 \right) \right] e^{-i\alpha/2} \sqrt{\frac{1}{V|D''(z_0)|}} \right\rangle_{(T, \mu=0)} \quad (4.4)$$

for large V . Here, $D''(z) = (d^2/dz^2) (N_f N_t \sum_{n=1}^{\infty} D_n z^n)$ and $D''(z_0) = |D''(z_0)| e^{i\alpha}$.

The chemical potential, i.e. the slope of the effective potential, is also evaluated by

$$\frac{\mu_q}{T} = \frac{-1}{V} \frac{\partial \ln \mathcal{Z}_C(T, \bar{\rho}V)}{\partial \bar{\rho}} \approx \frac{\left\langle z_0 \exp [V (N_f N_t \sum_{n=1}^{\infty} D_n z_0^n - \bar{\rho} z_0)] e^{-\frac{i\alpha}{2}} \sqrt{\frac{1}{V|D''(z_0)|}} \right\rangle_{(T, \mu_q=0)}}{\left\langle \exp [V (N_f N_t \sum_{n=1}^{\infty} D_n z_0^n - \bar{\rho} z_0)] e^{-\frac{i\alpha}{2}} \sqrt{\frac{1}{V|D''(z_0)|}} \right\rangle_{(T, \mu_q=0)}}. \quad (4.5)$$

This equation is similar to the formula of the reweighting method for finite μ_q . The operator in the denominator corresponds to a reweighting factor, and the chemical potential is an expectation value of the saddle point calculated with this modification factor.

We analyze the data used in the previous section. The Taylor expansion coefficients up to $O(\mu_q^6)$ are used. The volume $V = 16^3$ would be sufficiently large, and we assume a Gaussian distribution function for the complex phase of the reweighting factor, again. We find a saddle point z_0 numerically for each configuration, assuming z_0 exists near the real axis in the low density region of the complex μ_q/T plane. We use multi- β reweighting method [10] combining all data obtained at 16 points of β . Configurations are generated with the provability of the Boltzmann weight in Monte-Carlo simulations, however the important configurations will change when the weight is changed by the reweighting method. For such a case, the multi- β reweighting is effective, since the important configurations are automatically selected among all configurations generated at multi- β , and also this method is useful for the interpolation between the simulation points.

We plot the result of μ_q/T in Fig. 4 as a function of ρ/T^3 for each temperature. The dot-dashed line is the value in the free gas limit. As seen in Fig. 2 (left), the configurations do not distribute uniformly in the range of P which is necessary in this analysis, and correct results cannot be obtained if the important configurations are missing. At low temperature, the important value of P changes very much as ρ increases, therefore we plotted only the data when the expectation value of P is on the peaks of the histograms of P in Fig. 2 (left). The dashed lines are cubic spline interpolations of these data.

It is found from this figure that a qualitative feature of μ_q/T changes around $T/T_c \sim 0.8$, i.e. μ_q/T increases monotonically as ρ increases above 0.8, whereas it shows an s-shape below 0.8. This means that there is more than one values of ρ/T^3 for one value of μ_q/T below $T/T_c \sim 0.8$. This is a signature of a first order phase transition. The critical value of μ_q/T is about 2.5, which is consistent with the result in the previous section. Although further studies including justifications of these approximations used in this analysis are necessary for more qualitative investigation, this result also suggests the existence of the first order phase transition line in the (T, μ_q) plane.

References

- [1] C.R. Allton, *et al.*, *Phys. Rev. D* **66** (2002) 074507 [hep-lat/0204010].
- [2] C.R. Allton, *et al.*, *Phys. Rev. D* **68** (2003) 014507 [hep-lat/0305007].
- [3] C.R. Allton, *et al.*, *Phys. Rev. D* **71** (2005) 054508 [hep-lat/0501030].
- [4] S. Ejiri, arXiv:0706.3549.
- [5] J.B. Kogut and D.K. Sinclair, PoS(LAT2006)147 [hep-lat/0609041]; arXiv:0709.236.
- [6] D.E. Miller and K. Redlich, *Phys. Rev. D* **35** (1987) 2524.
- [7] A. Hasenfratz and D. Toussaint, *Nucl. Phys. B* **371** (1992) 539.
- [8] A. Alexandru, M. Faber, I. Horvath and K.-F. Liu, *Phys. Rev. D* **72** (2005) 114513 [hep-lat/0507020].
- [9] S. Kratochvila and P. de Forcrand, PoS(LAT2005)167 [hep-lat/0509143].
- [10] A.M. Ferrenberg and R.H. Swendsen, *Phys. Rev. Lett.* **63** (1989) 1195.